



HAL
open science

Coupled effects of spreading solvent molecules and electrostatic repulsions on the behavior of PS-b-PAA monolayers at the air-water interface

Zineb Guennouni, Michel Goldmann, Marie-Claude Fauré, Philippe Fontaine, Patrick Perrin, Denis Limagne, Fabrice Cousin

► **To cite this version:**

Zineb Guennouni, Michel Goldmann, Marie-Claude Fauré, Philippe Fontaine, Patrick Perrin, et al.. Coupled effects of spreading solvent molecules and electrostatic repulsions on the behavior of PS-b-PAA monolayers at the air-water interface. *Langmuir*, 2017, 33 (43), pp.12525-12534. 10.1021/acs.langmuir.7b02664 . hal-01612065

HAL Id: hal-01612065

<https://hal.sorbonne-universite.fr/hal-01612065>

Submitted on 6 Oct 2017

HAL is a multi-disciplinary open access archive for the deposit and dissemination of scientific research documents, whether they are published or not. The documents may come from teaching and research institutions in France or abroad, or from public or private research centers.

L'archive ouverte pluridisciplinaire **HAL**, est destinée au dépôt et à la diffusion de documents scientifiques de niveau recherche, publiés ou non, émanant des établissements d'enseignement et de recherche français ou étrangers, des laboratoires publics ou privés.

Article

Coupled effects of spreading solvent molecules and electrostatic repulsions on the behavior of PS-b-PAA monolayers at the air-water interface

Zineb Guennouni, Michel Goldmann, Marie-Claude Fauré, Philippe Fontaine, Patrick Perrin, Denis Limagne, and Fabrice Cousin

Langmuir, **Just Accepted Manuscript** • DOI: 10.1021/acs.langmuir.7b02664 • Publication Date (Web): 03 Oct 2017Downloaded from <http://pubs.acs.org> on October 4, 2017**Just Accepted**

“Just Accepted” manuscripts have been peer-reviewed and accepted for publication. They are posted online prior to technical editing, formatting for publication and author proofing. The American Chemical Society provides “Just Accepted” as a free service to the research community to expedite the dissemination of scientific material as soon as possible after acceptance. “Just Accepted” manuscripts appear in full in PDF format accompanied by an HTML abstract. “Just Accepted” manuscripts have been fully peer reviewed, but should not be considered the official version of record. They are accessible to all readers and citable by the Digital Object Identifier (DOI®). “Just Accepted” is an optional service offered to authors. Therefore, the “Just Accepted” Web site may not include all articles that will be published in the journal. After a manuscript is technically edited and formatted, it will be removed from the “Just Accepted” Web site and published as an ASAP article. Note that technical editing may introduce minor changes to the manuscript text and/or graphics which could affect content, and all legal disclaimers and ethical guidelines that apply to the journal pertain. ACS cannot be held responsible for errors or consequences arising from the use of information contained in these “Just Accepted” manuscripts.



Coupled effects of spreading solvent molecules and electrostatic repulsions on the behavior of PS-*b*-PAA monolayers at the air-water interface

Zineb Guennouni^{a,b,†}, Michel Goldmann^{*,a,c,d}, Marie-Claude Fauré^{a,c}, Philippe Fontaine^d, Patrick Perrin^{e,f}, Denis Limagne^a and Fabrice Cousin^{*,b}

^aSorbonne Universités, UPMC Univ Paris 06, CNRS-UMR 7588, Institut des NanoSciences de Paris, 4 place Jussieu F-75005 Paris, France

^bLaboratoire Léon Brillouin, CEA Saclay, 91191 Gif sur Yvette Cedex, France

^cFaculté des Sciences Fondamentales et Biomédicales, Université Paris Descartes, 45 rue des Saints Pères, 75006 Paris, France

^dSynchrotron SOLEIL, L'Orme des Merisiers, Saint-Aubin, BP 48, 91192 Gif-sur-Yvette, France

^eEcole Supérieure de Physique et de Chimie Industrielles de la Ville de Paris (ESPCI), ParisTech, PSL Research University, Sciences et Ingénierie de la Matière Molle (SIMM), CNRS UMR 7615, 10, Rue Vauquelin, F-75231 Cedex 05 Paris, France

^fSorbonne-Universités, UPMC Univ Paris 06, SIMM, 10, Rue Vauquelin, F-75231 Cedex 05 Paris, France

ABSTRACT: We describe the surface behavior of PS-*b*-PAA monolayers at the air/water interface using N,N-dimethylformamide (DMF) as spreading solvent. At low pH, when the PAA blocks are neutral, the surface pressure *versus* molecular area isotherm shows a pseudoplateau associated with the presence of remaining solvent spreading molecules in the monolayer, as we described in a former study (Guennouni *et al*, Langmuir, 2016). We show here that the width of the plateau decreases when increasing pH up to its complete disappearance at high pH, when PAA blocks are fully charged, although there still exist two regimes of compressibilities on the isotherm. A refined structural study at pH 9 combining Specular Neutron Reflectivity (SNR), Grazing-Incidence Small-Angle X-rays Scattering (GISAXS) and Atomic Force Microscopy (AFM) in liquid measurements show that: (i) PAA blocks are stretched in solution, as expected from polyelectrolyte brushes in osmotic regime; (ii) the system undergoes a spinodal decomposition during deposit at the air/water interface in presence of DMF. Upon compression, the Q_{xy}^* position of the peak associated with the spinodal structure remains almost constant but its intensity evolves strongly and passes through a maximum at intermediate pressures. This reveals two operating processes in the system: strong electrostatic repulsions between chains that prevent in-plane reorganizations and force such reorganizations to occur from the surface to the volume and progressive expulsion of the DMF molecules from the monolayer. These processes have antagonist effects on the intensity of the peak: the increase of the repulsions makes it more pronounced whereas the expulsion of solvent makes it vanish due to the loss of contrast.

INTRODUCTION

Monolayers of charged amphiphilic block copolymers at the air/water interface have a huge potential for applications because their physical properties can be monitored over a wide range through the tuning of electrostatic interactions in the aqueous subphase [1][2][3][4][5]. In particular, their further transfer onto solid substrate[6], if controlled, opens the way to the design of pH-responsive systems. In turn, the description of their surface behaviour is an intricate problem to address since many physicochemical parameters may influence the mechanisms driving such behaviour, namely the respective masses and hydrophilicity/hydrophobicity of the blocks, the choice of solvent spreading, the pH, ionic strength, and linear

charge density of the charged block that control the electrostatic interactions.

In this framework, we aim here at probing the concurrent influences of electrostatic interactions and solvent spreading effects on the surface behaviour of polystyrene-*b*-(acrylic acid) (PS-*b*-PAA) copolymers. This system is a tool of choice for such a study because it has at the same time a very hydrophobic anchor (PS) and a hydrophilic block whose pKa is located at intermediate pH (~ 4.7). The linear charge density of this block can thus be finely tuned by varying the pH from totally neutral up to fully charged, enabling to decouple influence of electrostatic effects on surface behaviour from other ones, contrarily to copolymers with strong polyelectrolytes blocks such as

1 poly(hydrogenated isoprene)-*b*-poly(styrene sulfonate)[3]
2 [4]. The neutral case makes it possible to compare with
3 PS-*b*-PEO whose behavior has been very well described in
4 the literature [7][8][9][10].

5 We first underline that finding a good spreading sol-
6 vent for PS-*b*-PAA is not easy considering the two blocks
7 different affinities, contrary to the case of PS-*b*-PEO or
8 PS-*b*-PMMA where the volatile chloroform can be used.
9 One often use spreading solvent formed by hydro-
10 philic–hydrophobic solvent mixtures which respective
11 concentrations can be adjusted to the relative weight of
12 each block [5][11][12][13]. However, the use of a pure sol-
13 vent guarantees the absence of possible biases, for exam-
14 ple related to differences in evaporation rate. To this aim,
15 the DMF, which dissolves both blocks, appears as a good
16 choice, although it presents the drawback to dissolve into
17 the aqueous subphase instead of being evaporated at
18 room temperature. Indeed, it is miscible with water, has a
19 high boiling point (153°C) and a low vapor pressure.

20 Surface pressure *versus* surface density isotherm of the
21 PS-*b*-PAA system for different pH of the subphase were
22 firstly presented by Currie *et al* using a 60% dioxane-40%
23 toluene solvent and for different pH of the subphase [5].
24 The main observed features are the following: at low pH,
25 the compression isotherm evidences a surface pressure
26 plateau usually associated to a first order transition of the
27 organic monolayer. This plateau is not observed anymore
28 at high pH and Currie *et al* associated it to a mushrooms-
29 brushes transition of the PAA block. Wang *et al* studied
30 these monolayers at pH 7 by BAM using DMF as solvent
31 [14]. They confirm the presence of the “pseudoplateau”
32 that they interpreted as a pancake to brush transition too,
33 although the PAA chains are likely to be totally charged at
34 such pH. They also observed by BAM an aggregation
35 process in the monolayer that they attributed to the DMF
36 slow dissolution in the subphase. However, the aggregates
37 where not recovered when observing the film by AFM
38 after transfer by the LB procedure. We note that the sam-
39 ples were dried for 24h before AFM measurement. The-
40 odoly *et al* [15] studied the microscopic structure of these
41 films by GISAXS at pH 11 using dioxane as solvent. There-
42 fore, micelles exist in the spreading solution as dioxane is
43 not a good solvent for PS. No pseudo-plateau was ob-
44 served at such high pH. The data have been interpreted
45 by the presence of hexagonally packed surface micelles
46 which dissociated into a brush under the film compres-
47 sion. Combining neutron reflectivity and GISAXS mea-
48 surements, we recently characterized the microscopic
49 structure of PS-*b*-PAA layer deposited from a DMF solu-
50 tion at the air/water interface [16]. Clearly, at pH 2, the
51 compression isotherm exhibits a surface pressure pseudo-
52 plateau. Our GISAXS results however demonstrated that
53 the PS-*b*-PAA monolayers were not homogenous but do
54 not form surface micelles. Moreover, by neutron reflectiv-
55 ity, we demonstrated that the PAA chains remain ad-
56 sorbed at the interface irrespective of the pressure and
57 never reach the brushes configuration. This pointed out
58 the influence of the spreading solvent as the structure of
59 the monolayer was different from those described by

Currie *et al*. To explain our results at low pH, we have
proposed a new model based on the possibility that some
DMF molecules (from the spreading solvent) remain
adsorbed within the monolayer at low surface pressure.
These molecules are desorbed below the interface when a
critical surface pressure is reached. This corresponds to
the onset of the plateau on which the DMF molecules are
continuously desorbed under compression. The end of
the plateau corresponds to the full expulsion of the DMF.
However, at higher pH, when PAA blocks are fully
charged [11], the possible formation of brushed may
strongly change the behavior of the monolayer. This
prompted us to study the isotherm of the system on a
large pH range and to make a proper structural study by
SNR and GISAXS at pH 9 complemented by AFM exper-
iments on transferred film. In this latter case, we insured
that the organic film has always been in liquid environ-
ment.

MATERIALS AND METHODS

Materials. Polystyrene-poly(acrylic acid) diblock co-
polymer PS_D-*b*-PAA were provided by Polymer Source
Inc., Canada. It consists of 33 deuterated styrene repeti-
tion units (Mn=3500 g/mol) and 143 acrylic acid repetition
units (10800 g/mol) with polydispersity index, Pi=1.12.

Silicon wafers (thickness= 281 ± 25 μm, orientation =
(100), no dopant, roughness= 5 Å) were purchased from
ACM (France).

Isotherms. The copolymers were dissolved in N,N-
dimethylformamide (DMF) to form spreading solutions of
typical concentrations of order of 2 · 10⁻⁴ mol/L. In a previ-
ous publication, we checked the total solubilization of the
copolymer chains in DMF [16]. A few microliters of the
solution were deposited drop by drop with a micro-
syringe (Hamilton) onto the air/liquid interface of a
Langmuir trough equipped with 1 or 2 movable barrier(s)
for film compression. After deposit, it was waited for a
minimum time of 10 minutes to let the monolayer equili-
brate before starting to compress. The surface pressure
was measured according to the Wilhelmy plate method.
The plate is made of filter paper and the measurement
device is a microbalance from Riegler&Kirstein GmbH
(Germany). The subphase consisted of Milli-Q Millipore
ultra-pure water (18.2 MΩ.cm) into which either HNO₃ or
NaOH (Sigma Aldrich, purity better than 98 %) was add-
ed to set the pH at the desired values. The temperature
was regulated at 18 ± 0.5 °C using a circulating water bath.
Prior to the deposit of each monolayer, the Teflon® trough
was cleaned with Hellmanex® and rinsed several times
with ultra-pure water. Before any experiment we checked
that the subphase surface was not polluted. Each iso-
therm was performed three or four times to check the
reproducibility of the results. It was always very good in
all the conditions probed.

All isotherms were performed at a constant speed com-
pression of 35 Å²/molecule/min. The typical time of iso-
therm cycle (compression-expansion) is about 1h15. The
speed compression has no influence on the isotherm. We

checked it by performing isotherms at two very different compression speeds, 3 $\text{\AA}^2/\text{molecule}/\text{min}$ and 400 $\text{\AA}^2/\text{molecule}/\text{min}$ (10 times slower and faster than the usual speed), and we did not detect any change in the isotherms (data not shown).

We also performed some experiments where pH was changed in situ from pH 2 to pH 9, or the reverse. For such experiments, we used the following protocol. A complete first cycle of compression-expansion isotherm of the copolymer monolayer was first carried out at the initial pH. To modify the pH of the subphase, the copolymer film was then compressed again a second time until the complete stop of the barriers of the trough. Beyond the two barriers, the necessary amounts of HNO_3 (or NaOH) were gradually added to change pH to the desired value. The monolayer was then completely expanded and left to stand. After about ten minutes, a complete new cycle of compression-expansion isotherm was performed at the new pH. In order to ensure the reproducibility of the results, all the reversibility measurements were repeated several times, varying different parameters such as the monolayer rest time after the pH change and the number of isothermal cycles performed before and after the pH change.

Specular Neutron Reflectivity (SNR). Specular neutron reflectivity experiments were carried out in situ on a Langmuir trough, thermalized at 18°C , on the horizontal time-of-flight reflectometer EROS at LLB [17]. The Q_z -range that was probed lied between 0.008 and 0.18\AA^{-1} , with a $\Delta Q/Q$ resolution of ~ 0.12 . The incoherent scattering was measured independently and subtracted from the SNR curves before any modelling. All experimental details can be found in ref [16] or in *Supporting Information*.

Two conditions of subphase contrasts were thus used to take benefit from the fact that the PS part of the copolymer was deuterated : (i) a mixture of 67%/33% $\text{H}_2\text{O}/\text{D}_2\text{O}$ that has a Scattering Length Density (SLD) N_B of $1.7 \cdot 10^{-6} \text{\AA}^{-2}$ and matches exactly the SLD of the PAA chains, making only the PSD part observable; (ii) pure deuterated water ($N_B = 6.39 \cdot 10^{-6} \text{\AA}^{-2}$) which is very close to the SLD of deuterated polystyrene ($6.5 \cdot 10^{-6} \text{\AA}^{-2}$) makes the PAA part observable. The SLD of the hydrogenated DMF used for the deposit is $0.70 \cdot 10^{-6} \text{\AA}^{-2}$.

Data were analyzed by model fitting using the Parratt formalism. The interface was described by a series of layers, each of them being characterized by a thickness, a scattering length density and a roughness. The experimental resolution of the spectrometer was taken into account in the calculation.

Grazing Incidence Small angle X-ray Scattering (GISAXS). GISAXS measurements were performed on a dedicated PTFE Langmuir trough at the ID10B beamline at the ESRF synchrotron source (Grenoble, France). All experimental details, as well as the respective electronic scattering length densities of the component can be found in *Supporting Information* or in ref [16]. The surface pressure was kept constant during a scan.

AFM measurement in liquid mode after transfer of the monolayer on hydrophobic substrates. Silicon wafers substrates were first cleaned by an immersion in an active "piranha" solution (30% H_2O_2 /70% H_2SO_4 , highly corrosive), extensively rinsed with Milli-Q water and dried with a nitrogen flow. They were immediately silanized with a mixture of Octadecyltrichlorosilane (OTS) at a concentration of 0.15 vol% in anhydrous toluene for 2h at ambient temperature [18]. This treatment allowed us to obtain highly hydrophobic substrates for the further transfer of the PS-b-PAA monolayer.

Such transfer was achieved either by the Langmuir-Schaefer technique or Langmuir-Blodgett technique, using the same Langmuir trough as for the isotherm. For such purpose, new protocols were designed to transfer the PS-b-PAA monolayer at a settled pressure onto the hydrophobic wafer that ensures that sample stays maintained at every step within the aqueous buffer up to their measurement by AFM. This avoided the damaging of the deposited copolymers monolayer, a mandatory prerequisite given that dewetting effects are usually observed for such PS-b-PAA monolayers [19]. These protocols are presented in *Supporting Information*.

Finally, the structure of the PS-b-PAA monolayer was probed by an Atomic Force Microscope (AFM, nanoscope 3100, Veeco) in liquid environment in the contact mode.

RESULTS

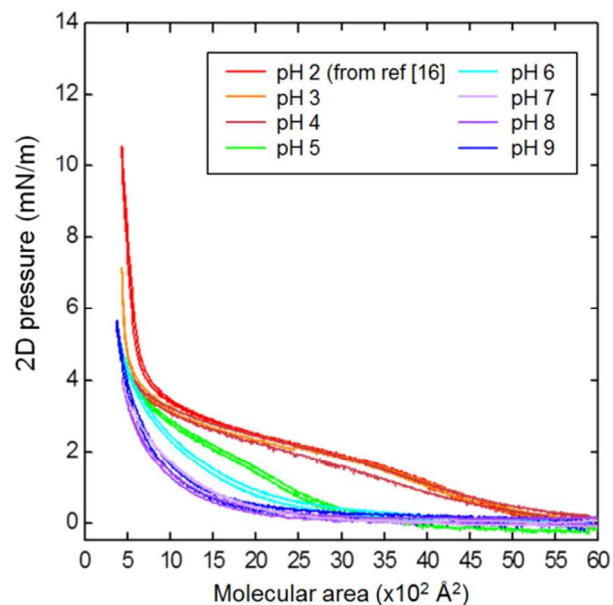


Figure 1: Surface pressure isotherm cycles of PS-b-PAA copolymers at different pH, at $T = 18^\circ\text{C}$ and at a compression rate of $35 \text{\AA}^2/\text{mol}/\text{min}$ with a deposited volume such as the initial molecular area corresponds to $6000 \text{\AA}^2/\text{molecule}$. The data at pH 2 come from reference [16] and have been measured exactly in the same conditions.

Isotherms

In order to obtain a full understanding of the behavior of the PS-b-PAA amphiphilic diblock copolymers at the

air/liquid interface, we have characterized the PS-*b*-PAA monolayers by using the Langmuir technique on a wide range of pH lying from pH 3 to pH 9 since the pK_a of the carboxylic groups of PAA is 4.7. The same copolymers solution was used and this completes the data we already obtained at pH 2 in ref [16] (Figure 1).

Stability and reproducibility of the isotherms.

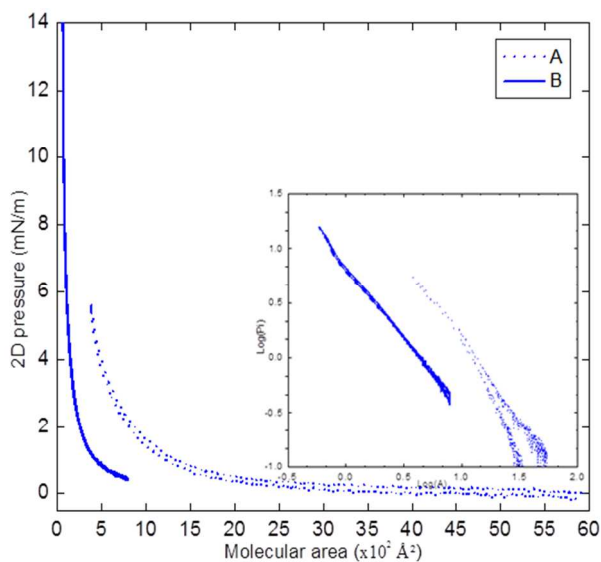


Figure 2. Surface pressure isotherm cycles of PS-*b*-PAA copolymers film formed at pH 9 (concentration of spreading solution = 2×10^{-4} mol/L, $T = 18$ °C) and starting from a maximal area of: A: $6000 \text{ \AA}^2/\text{molecule}$; B: $800 \text{ \AA}^2/\text{molecule}$. Inset shows the same data in log-log scale.

When the solution is deposited onto the surface, a monolayer is formed, as shown by Wang *et al* [14] by Brewster microscopy, although some part of material is lost in the subphase because the DMF spreading solvent is miscible with water. Although this loss of material is negligible at low pH when the PAA chains are neutral [16], it becomes important at high pH when the PAA chains are charged and thus very hydrophilic. This raises the question of the correct area per molecule on the isotherm, which is usually calculated from 3 experimental parameters making the hypothesis that all material is deposited on the surface: the concentration of the spread solution, the volume of deposited solution and the available surface of the air/water interface on the trough. Indeed, if one of these parameters changes, the calculation becomes inaccurate. This is illustrated in Figure 2 which shows two isotherms performed on the same trough and obtained with a given solution at a concentration of 2×10^{-4} mol/L with two different deposited volumes. Although the shape of the isotherm remains similar (see inset of Figure 2), the limit area and lift off vary indicating a greater loss of material in the case of the largest deposited volume since the isotherm appears shifted towards low molecular area. At least, the correct reliable parameter defining the film state is the surface pressure value (and the temperature of course), and results will be later discussed as function of such parameter. In the following, we

have decided to present the areas per molecule calculated as if no material was lost in the subphase but we remind the reader that they are only effective values.

The two isotherms of figure 2 were obtained with the conditions that we used for the different experiments of the paper. The maximal area of $6000 \text{ \AA}^2/\text{molecule}$ was those we use for probing the influence of pH (Figure 1). It was chosen to allow a proper comparison with the isotherm at pH 2 of reference [16]. The maximal area of $800 \text{ \AA}^2/\text{molecule}$ was used for GISAXS and NR measurements. It was chosen to optimize measurements with the Langmuir trough available at the large facilities.

Influence of pH on isotherms. Once a monolayer of PS-*b*-PAA was deposited, we waited at least 10 minutes to insure the removal of DMF excess. Several successive cycles of compression and expansion were then performed on the monolayer. At the lowest pH (2 to 4), the PS-*b*-PAA copolymers form a stable monolayer at the interface, all isotherms are reversible upon decompression and superimpose without hysteresis after several cycles as previously observed [16] at pH 2. On the contrary, at high pH, when the PAA chains are charged, the isotherms cycles are progressively shifted very slightly toward the smaller molecular area and present a weak hysteresis, without markedly altering the shape of the isotherm (see Figure S1.1 that shows 3 cycles of compression/expansion at pH 9 in *supporting information*). This probably results from a very limited loss of some copolymers in the aqueous subphase.

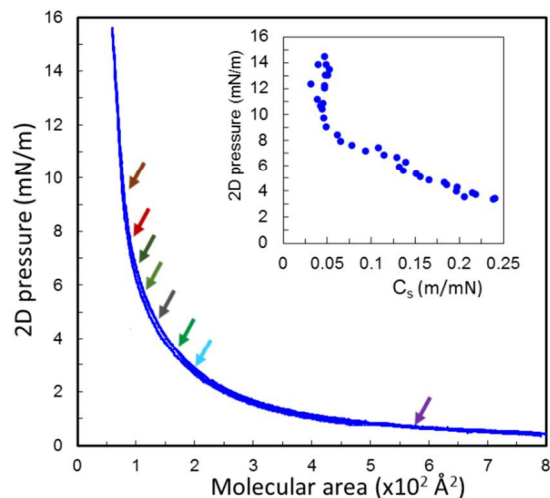


Figure 3. Surface pressure isotherm cycles of PS-*b*-PAA copolymers starting from a maximal area of $800 \text{ \AA}^2/\text{molecule}$ at pH 9 and $T = 18$ °C (conditions used for GISAXS and SNR measurements). The different arrows correspond to the different points of GISAXS and SNR measurements. The colors code is respected for GISAXS and SNR figures. Inset: 2D pressure *versus* compressibility C_s .

When the pH of the subphase varies from 2 to 9 (Figure 1), the shape of the isotherm progressively changed with

three typical behaviors, which point out the role of electrostatics : (i) At low pH ($\text{pH} < 4$), the PAA chains are neutral and one recovers the “pseudo-plateau” as in previous publications at about 3 mN/m surface pressure [5] [16]; (ii) when the pH increases to intermediate values ($4 \leq \text{pH} \leq 7$), the width of the pseudo-plateau gradually decreases continuously, the most important changes occurring at $\sim \text{pH} 5$, *i.e.* in the vicinity of the pK_a of the PAA chains; (iii) finally, at high pH ($\text{pH} > 7$), the PAA chains are fully charged and the pseudoplateau is no longer observed. In this last regime, the surface pressure remains almost null at large molecular areas down to a molecular area, and then increases upon further compression. The lack of pseudoplateau at pH 9 was interpreted by Currie *et al* [5] as the existence of only one PAA regime, the brush one, at every surface pressure due to the strong electrostatic repulsions between charged PAA blocks.

We remind that we demonstrated that the pseudoplateau observed at low pH was associated to the expulsion of DMF solvent from the monolayer. At intermediate pH value, this regime of high isothermal compressibility, *i.e.* $C_s = \left(-\frac{1}{A} \frac{\partial A}{\partial \pi}\right)_T$, is still present but the value of compressibility taken at the middle of the pseudoplateau, progressively decreases. It indicates that some repulsions counteract either the dissolution of the DMF, either the in-plane reorganizations of the systems that occur in this “expelling regime”. Thereby, the presence of such repulsions, presumably of electrostatic origin, reduces the width of the plateau. Ultimately, at high pH, although the pseudoplateau seems to have disappeared at first glance, the two regimes can be still identified when calculating C_s (see inset of Figure 3). The change occurs at a surface pressure of about 6.5 mN/m (Figure 3). It finally appears that there are not two distinct behaviours at low pH and high pH, but the different faces of the same given problem with specific effects arising from electrostatic repulsions between PAA blocks once they are charged.

In situ change of the pH of the subphase. We have also probed the evolution of the isotherm when changing *in situ* the pH of the subphase in order to pass from uncharged blocks at pH 2 to charged blocks at pH 9, and *vice versa*. Isotherms are shown in Figure SI.2 in *supporting information*. When passing from pH 2 to pH 9, one recovers an isotherm which shape is identical to those obtained when deposited at pH 9, although it is shifted towards large molecular areas. This shift results from the fact that the loss of materials at pH 9 is obviously more important than at pH 2. When passing from pH 9 to pH 2, the isotherm exhibits the pseudo-plateau at the same surface pressure as usually observed but its width has decreased by half. This shows that there was less DMF solvent remaining in the monolayer formed at pH 9 than at pH 2. These experiments demonstrate that the deposit conditions have a large impact with respect to the amount of lost materials and/or of trapped solvent but that the behavior of the system is reversible upon pH changes once monolayer is formed.

Specular Neutron Reflectivity

The sample was probed at three surface pressures (0.8 mN/m , 3.8 mN/m , 8 mN/m) by SNR measurements on an aqueous subphase at pH 9 in the two contrasts conditions. The different measurements points are indicated by arrows on the isotherm of Figure 3. The Fresnel curve, *i.e.* the SNR signal from the pure subphase, was systematically measured first. The layer was then deposited, first compressed up to 8 mN/m to check that one recovers the isotherm and expanded up to large molecular area. Then it was re-compressed again for measurements. All measurements were performed at constant surface pressure. For all of the three surface pressures the experimental SNR curves markedly differ from the Fresnel one, contrarily to what was observed at pH 2 [16].

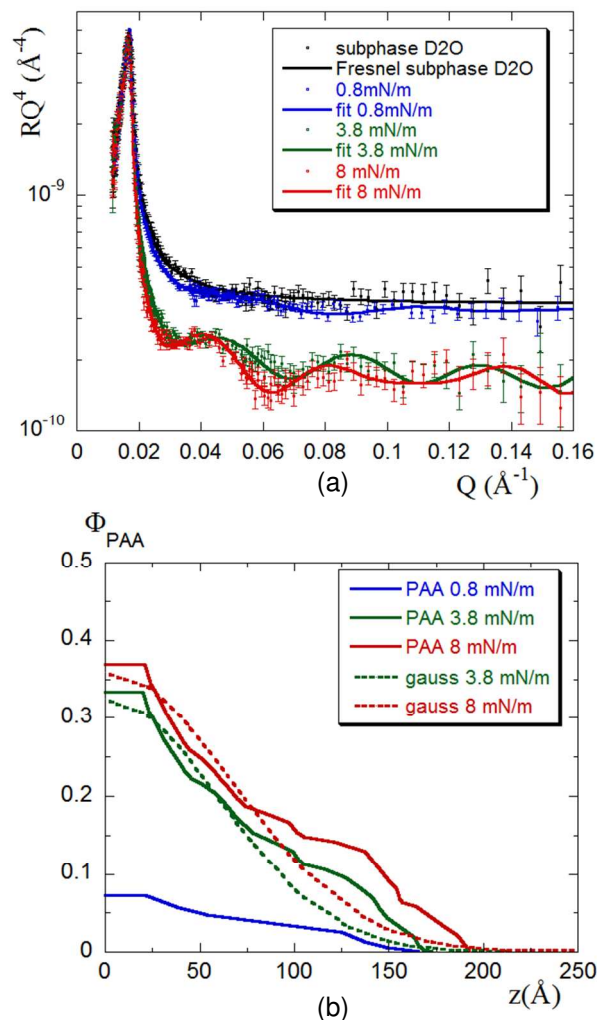


Figure 4. (a) SNR of the single subphase (100% D_2O) at pH 9 and $T = 18 \text{ }^\circ\text{C}$, covered by a $\text{PS}_D\text{-}b\text{-PAA}$ copolymer monolayer at various surface pressures. Continuous lines correspond to the best fits. (b) $\Phi_{\text{PAA}}(z)$, as obtained from the fits. The dashed lines correspond to a Gaussian profile (see text).

For the 100% D_2O subphase contrast, they present a lower intensity than the Fresnel ones and some interference Kiessig fringes (see results in Figure 4 that are displayed in the Fresnel representation ($R(Q_z)Q_z^4$ versus

$f(Q_z)$). In such contrast (PS_D almost contrast-matched), the contribution to the scattering originates essentially from the PAA blocks (SLD of $1.7 \cdot 10^{-6} \text{ \AA}^{-2}$), as well as some potential DMF within the layer (SLD of $0.7 \cdot 10^{-6} \text{ \AA}^{-2}$). These spectra show that the PAA blocks are stretched in water, since a swollen PAA layer in D_2O presents a lower mean SLD than the one of pure D_2O , and form a rather thick layer at the interface because of the strong electrostatic repulsions induced by the deionization of the carboxyl groups.

The Kiessig fringes are not very marked at 0.8 mN/m, suggesting that the surface density of PAA remains low, whereas they are very marked at 3.8 mN and at 8 mN/m, suggesting a significant densification of the PAA layer. Moreover, the fringes are progressively shifted towards low Q from 0.8 mN/m to 8 mN/m, *i.e.* an overall increase of the thickness of the layer, revealing a thicker layer associated to a stretching of chains upon compression.

The SLD profiles $N_B(z)$ have been obtained from the best fits of the experimental data. These profiles have been then converted into $\Phi_{PAA}(z)$ profiles considering only PAA, PS_D and D_2O and are shown on Fig 4.b. The potential presence of DMF would contribute to $N_B(z)$ due to its low SLD. The $\Phi_{PAA}(z)$ profiles are therefore probably not accurate in terms of absolute volume fraction. In particular, $\Phi_{PAA}(0)$ must be overestimated. Despite this, the shape of the profiles and its evolution due to compression are representative. At 0.8 mN/m, $\Phi_{PAA}(z)$ is very low. The PAA chains form a layer of thickness of 170 \AA , which is well below the fully stretched length of the PAA blocks (about 350 \AA , taking $N = 143$ and a monomer size of 2.5 \AA). When the film is compressed up to 3.8 mN/m, the thickness of the PAA layer only slightly increases, but its surface density increases greatly. At 8 mN/m, the profile is very similar to the one at 3.8 mN/m, with a slight increase of both the surface density and the thickness. Please note that for this last pressure $\Phi_{PAA}(z)$ is practically accurate since the DMF is fully expelled (see discussion). The shape of the two dense profiles has been compared to a Gaussian function $\Phi(z) = \Phi_0 \exp(-z^2/l^2)$ where Φ_0 is the density at the surface and l is the specific length of the profile, as expected for polyelectrolyte brushes in the osmotic regime; *i.e.* high surface density and low ionic strength [20][21][22][23]. They are in good accordance with such Gaussian behaviour (with respectively $\Phi_0 = 0.325$ and $l = 85 \text{ \AA}$ at 3.8 mN/m and $\Phi_0 = 0.36$ and $l = 95 \text{ \AA}$ at 8mN/m) up to a distance from the interface of $\sim 100 \text{ \AA}$. At further distance, there is an excess of PAA chains. This excess can be interpreted by the diving of some copolymers from the interface to the volume under the effect of the increase in surface pressure.

Figure 5 shows the SNR curves for the 67%/33% H_2O/D_2O subphase contrast (PAA blocks are contrast-matched), where the PS_D anchoring blocks, that potentially contain some DMF, are probed. At low pressure (0.8 mN/m), there is already a noticeable layer at the surface since the intensity of the SNR curve is much higher than the Fresnel one. This SNR curve can be modelled with a

single layer of 20 \AA with a SLD of $2.5 \cdot 10^{-6} \text{ \AA}^{-2}$. These values are the ones enabling the modelling with the lowest χ^2 , even so several profiles allow to fit the data for such a low thickness within errors bars with thickness/SLD pairs lying in the range (18 \AA - 22 \AA and $2.2 \cdot 10^{-6} \text{ \AA}^{-2}$ - $2.8 \cdot 10^{-6} \text{ \AA}^{-2}$). This enables to determine Φ_{PSD} by assuming that PSD blocks lay within water at the interface, a reasonable assumption given that the PAA chains are solvated and that copolymers form surface aggregates (see next part). The potential presence of DMF in the PS layer may affect the determination of Φ_{PSD} but such modification is weak due to contrast issues. Indeed, one gets $\Phi_{PSD} \sim 0.16$ by considering that the layer does not contain DMF, and $\Phi_{PSD} \sim 0.19$ if there remains 40%v/v of DMF within the PS, as observed in bulk on PS-b-PAA copolymer micelles [24]. This low volume fraction is in accordance with the large molecular area of the layer at such a surface pressure.

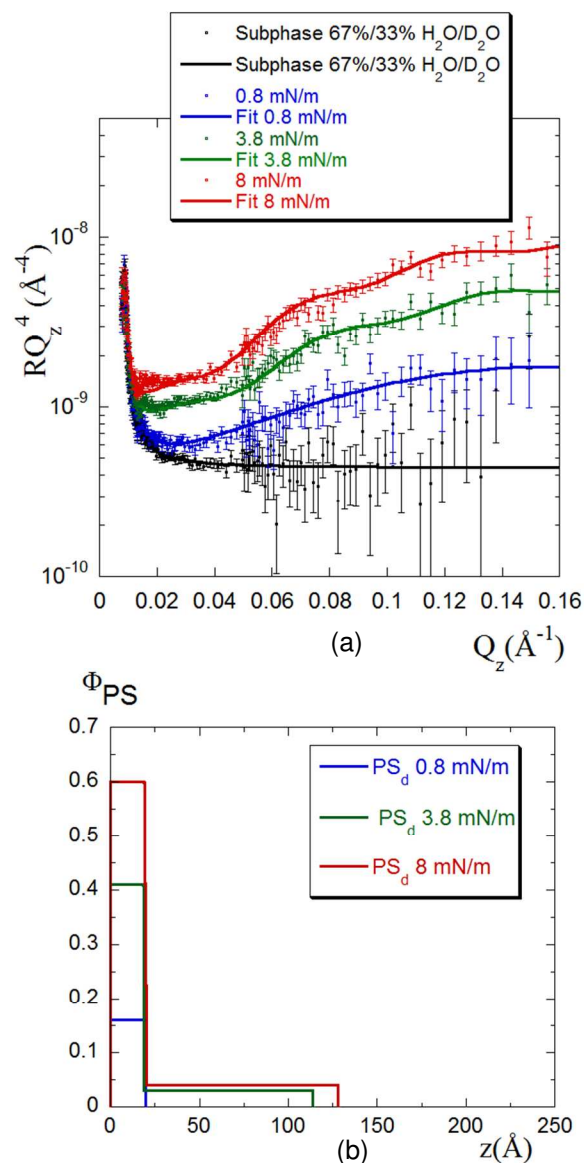


Figure 5. (a) SNR of the single subphase contrast (67%/33% H_2O/D_2O) at pH 9 and $T = 18 \text{ }^\circ\text{C}$, covered by a PS_D -b-PAA copolymer monolayer at various surface pressures. Con-

tinuous lines correspond to the best fits. (b) $\Phi_{\text{PS}}(z)$, as obtained from the fits.

When the surface pressure is increased up to 3.8 mN/m, the intensity of the SNR curve strongly increases, evidencing a large enrichment in PSD at the surface. The shape of the SNR curve also changes, as some damped fringes are present at low Q_z . This reveals that a second layer with a large thickness appears below the dense thin anchoring layer of PSD at the surface. It has not been possible to model the SNR curve by a single layer and a two-layers model has been used to fit the experimental SNR curve (see figure SI.3 in *supporting information* that compares models with respectively 1 or 2 layers). The dense small layer has a thickness of 19 Å and a SLD of $3.7 \cdot 10^{-6} \text{ \AA}^{-2}$, ($\Phi_{\text{PSD}} \sim 0.4$) and the second layer is $\sim 100 \text{ \AA}$ thick with an SLD of $1.85 \cdot 10^{-6} \text{ \AA}^{-2}$, that gives Φ_{PSD} of around 0.03 (see Figure 5.b). When the surface pressure layer is increased up to 8 mN/m, the same behaviour is recovered. The thickness of first layer remains at 19 Å but its SLD increases to $4.7 \cdot 10^{-6} \text{ \AA}^{-2}$, *i.e.* a Φ_{PSD} value of 0.6. The second layer has around the same thickness (110 Å) and the same SLD ($1.9 \cdot 10^{-6} \text{ \AA}^{-2}$) as for 3.8 mN/m. As the evaluation of Φ_{PSD} is poorly affected by DMF for such contrast, it has been possible to check the consistency of the model by verifying that the mass of PSD remains constant at the interface. This mass is proportional to $\Gamma \cdot A$, where Γ is the excess mass and A the molecular area. Γ is proportional to $\int_0^{\infty} \Phi_{\text{PSD}}(z) dz$. The values for all surface pressures are reported in table SI.1, and demonstrate such mass conservation (see *supporting information*).

The appearance of an additional PSD layer at surface pressure ranging between 0.8 mN/m and 3.8 mN/m is in accordance with the behaviour of the PAA blocks, whose profiles also deviate from those of pure osmotic brushes at the same pressures. This confirms that part of the PS blocks dive into the volume under the effect of the increase of the surface pressure, a behaviour that was not observed at low pH [16].

Grazing Incidence Small angle X-ray Scattering

The in-plane structure of the system at pH 9 was probed by GISAXS from 3 mN/m to 10 mN/m. A strong correlation peak readily marked is present on the GISAXS pattern up to a surface pressure of 8 mN/m that disappears for highest pressures. It arises from a surface scattering as it appears as a vertical line on the Q_{xy} - Q_z 2D pattern (Figure 6.a). A similar correlation peak was observed at pH 2 and originates from the presence of DMF trapped in PS. Indeed DMF has an electronic scattering length density very different from those of water, PS and PAA (see *supporting information*). Here also the correlation peak arises from the presence of DMF. The characteristic thickness of the scattering layer is $\sim 10 - 20 \text{ \AA}$, as derived from the rodscan analysis at Q_{xy}^* which corresponds to the maximum intensity of the correlation peak

(*supporting information*). This thickness value is of the same order as the PS thickness determined from SNR.

The 2D pattern was integrated along Q_z from 0 to 0.2 \AA^{-1} to obtain $I(Q_{xy})$. The result for different surface pressures is shown in Figure 6.b. At low surface pressure, the position Q_{xy}^* of the correlation peak is located about $\sim 0.031 \text{ \AA}^{-1}$, which corresponds to $\sim 190 \text{ \AA}$ in direct space ($2\pi/Q_{xy}^*$). This characteristic distance is large so it can only result from the formation of surface aggregates. It is however notably lower than those obtained at pH 2 (that lay in the $300 \text{ \AA} - 450 \text{ \AA}$ range [16]). Moreover, it appears that this value remains almost fixed upon compression while its intensity varies strongly.

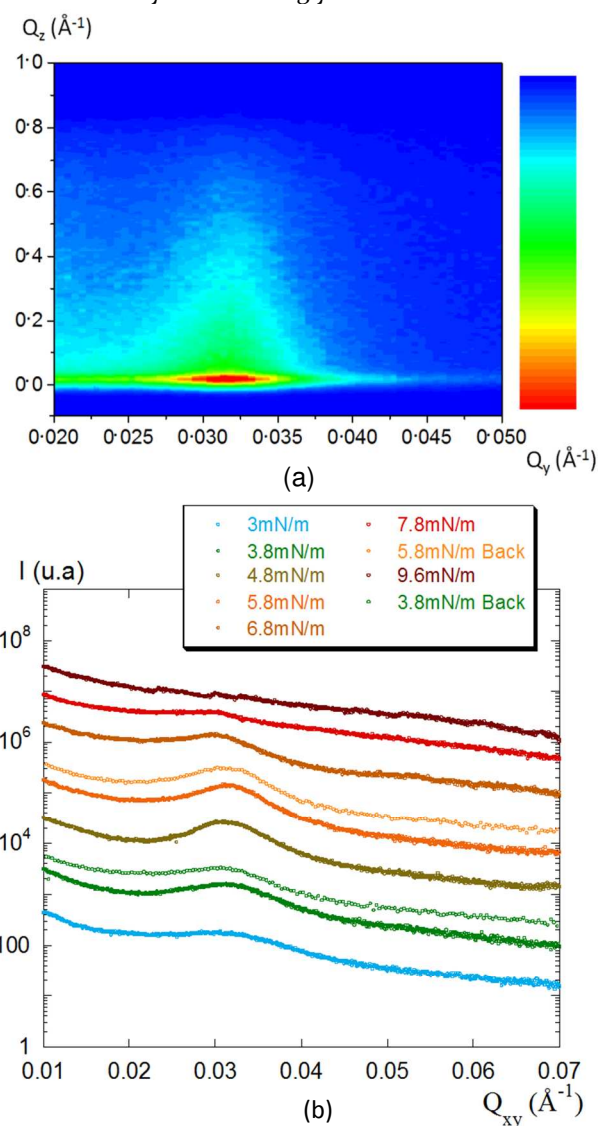


Figure 6. (a) Typical 2D GISAXS pattern for a PSD-b-PAA monolayer at 5.8 mN/m and $T = 18^\circ\text{C}$; (b) Integrated X-ray scattered intensity I versus Q_{xy} for a PSD-b-PAA monolayer at different surface pressures. Each curve is shifted for clarity by a factor 3 with respect to the previous curve. An example of reproducibility is presented at 5.8 mN/m and 3.8 mN/m, back indicating the expansion cycle.

In order to get a more quantitative description of the correlation peak, $I(Q_{xy})$ has been modelled by a Gaussian

function, as we formerly did for the pH 2 case in ref [16], to extract both its intensity and its position Q_{xy}^* (see supporting information). Data are reported in figure 7. Two regimes clearly appear depending on the surface pressure, the crossover between them corresponding to the difference of compressibility identified on the isotherm.

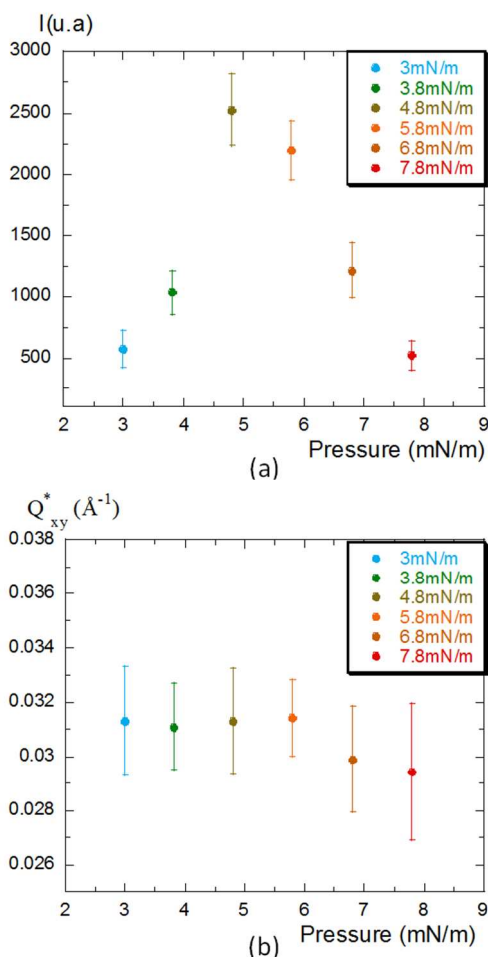


Figure 7. (a) Intensity of the correlation peak as function of surface pressure, as obtained from a simple modelling of the correlation peak by a Gaussian; (b) Q_{xy}^* as function of surface pressure.

In the regime of low surface pressures (3 mN/m – 5.8 mN/m), Q_{xy}^* has a constant value of 0.031 \AA^{-1} upon compression, *i.e.* the characteristic distance d^* does not vary (Figure 7.b). This dismisses the possible formation of surface micelles since d^* would scale with the square of the molecular area $A^{1/2}$. At the same time, the intensity of the peak strongly increases and reaches a maximum between 4.8 mN/m and 5.8 mN/m. These results, similar to first order transition, indicate a strong reorganization of the nanostructures at the interface during compression. The fact that d^* does not vary upon a decrease of molecular area A is *a priori* counterintuitive. Nevertheless, it can be consistent with a transfer of material from the interface to the volume without change of the interface structure during the compression of the film.

In the regime of large surface pressures (5.8 mN/m – 9.6 mN/m), the situation changes noticeably, which points out a structural reorganization of the surface. First, the correlation peak is progressively and slightly shifted towards low Q upon compression, *i.e.* largest distances in real space, from the value 0.031 \AA^{-1} at 5.8 mN/m up to 0.029 \AA^{-1} at 8 mN/m. Second, after the intensity of the correlation peak reached a maximum between 4.8 mN/m and 5.8 mN/m, it decreases up to complete disappearance above 8 mN/m. Such a disappearance can be explained by the expulsion of DMF from the surface aggregates. Indeed, the behaviour is reminiscent from what was observed at pH 2 where the peak disappeared when passing from the regime of high compressibility to low compressibility because of the loss of electronic contrast between aggregates and their surrounding vicinity when the DMF is fully expelled.

AFM in liquid

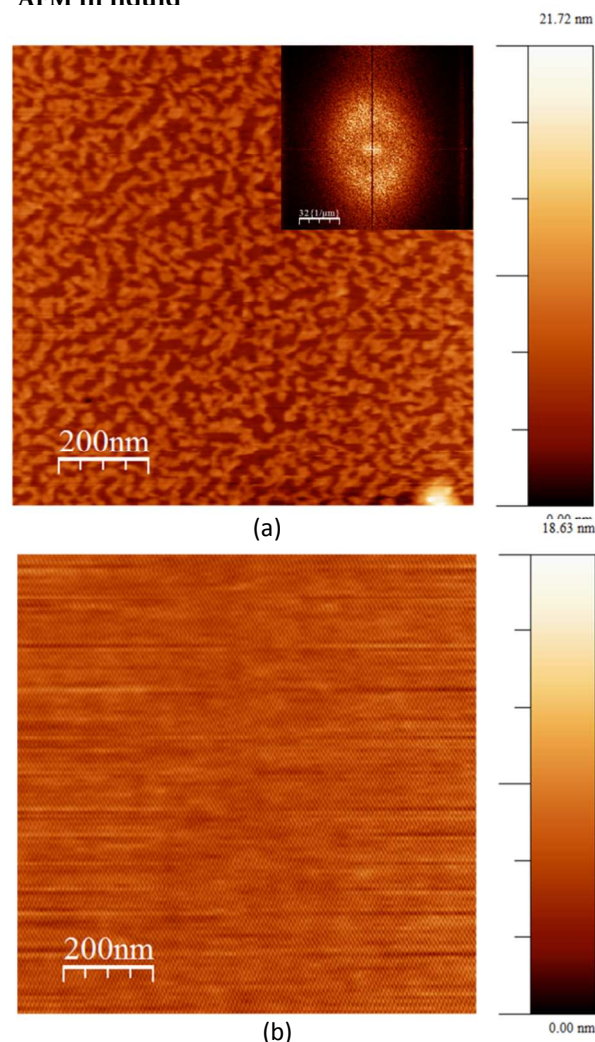


Figure 8. Topographic AFM pictures ($1 \mu\text{m} \times 1 \mu\text{m}$) in liquid medium of a monolayer of PS-*b*-PAA copolymers formed at the air-water interface at pH = 9 and transferred onto hydrophobic silicon wafers. (a) Deposit at 3.8 mN/m. Inset is a corresponding FFT transform of the picture. (b) Deposit at 14 mN/m.

1 We succeeded in transferring the monolayer on highly
2 hydrophobic substrates at pH 9, which demonstrates that
3 the outer layer of the monolayer was hydrophobic when
4 PAA blocks are charged. Figure 8 presents AFM images in
5 contact mode in liquid for 2 different surface pressures at
6 3.8 mN/m, and 14 mN/m. At 3.8 mN/m, one clearly ob-
7 serves an in-plane surface structure with a marked corre-
8 lation size, which corresponds to the structural feature
9 obtained from a spinodal decomposition. The thickness
10 variation range is ~ 50 Å. A 2D Fast Fourier Transform
11 of the picture at 3.8 mN/m gives a maximum at ~ 250 Å, of
12 the order of what is obtained with GISAXS experiments
13 (see inset of Figure 8.a). At 14 mN/m, the image appears
14 featureless, in agreement with the absence of correlation
15 peak in GISAXS experiments. For such a pressure, a hole
16 was made with the AFM tip within the monolayer to
17 check the presence of a real homogeneously layer onto
18 the surface (see Figure SI.7 in supporting information).

19 Since the SNR measurements showed that the PAA
20 blocks are stretched in water, the question arises of the
21 origin of the thickness variations on the monolayer trans-
22 ferred at 3.8 mN/m. This may be related to variations in
23 composition of the zones leading to stiffness variations
24 and thus to a change in the response of the tip of the AFM
25 when it interact with the surface. The thick areas may be
26 associated with DMF swollen PS chains and solvated PAA
27 chains while the thin ones are associated only with the
28 solvated PAA chains. When the DMF is expelled from the
29 monolayer (14 mN/m), we observe only one single homo-
30 geneous zone, which is associated with a layer composed
31 solely of PS and PAA chains.

32 DISCUSSION

33 Based on the combined structural information from
34 SNR, GISAXS and AFM measurements, Figure 9 proposes
35 a synoptic scheme of evolution of the monolayer over a
36 cycle of compression/expansion deposited on a pH 9
37 subphase. Contrary to the pH 2 case, there is a thick PAA
38 layer for all surface pressures, in agreement with a brush
39 configuration of the charged PAA block. Concerning the
40 PS block, there is a thin layer at large surface area which
41 gets denser under compression with the apparition of a
42 second buried layer, thick and of low density, when the
43 surface pressure reaches 3.8 mN/m. We interpret these
44 results by the diving of some copolymers below the mono-
45 layer when the surface pressure is high enough.

46 The GISAXS and AFM experiments reveal that the in-
47 plane microstructure is not homogeneous between 3
48 mN/m and 8 mN/m. Indeed, the AFM image is similar to
49 the one expected in case of a spinodal decomposition.
50 The in-plane typical distance d^* obtained at 3 mN/m
51 remains constant upon compression up to about 5 mN/m
52 while it GISAXS intensity increases continuously. At
53 higher surface pressure, this intensity starts decreasing
54
55
56
57
58
59
60

and vanishes at 8 mN/m as the d^* slightly increases. The-
se results can be interpreted by the combination of the
two phenomena: (i) the immersion of some PS-b-PAA
copolymer chains with increasing surface pressure; (ii) the
desorption of some DMF solvent molecules from surface,
but at a different surface pressures than observed at pH 2.
Indeed, up to 5 mN/m, domains with fixed DMF concen-
tration remain at the interface. Increasing the surface
pressure by compressing the layer induces the release of
some PS-b-PAA chains from the interface to the volume,
without changing significantly the DMF concentration
within the layer as well as the monolayer structure. At
higher surface pressure (> 6 mN/m), the second regime
of compressibility is reached: the remaining DMF mole-
cules are finally expelled within the subphase like liquid
molecules are expelled from a compressed sponge. This
leads to a variation of the surface concentration inducing
simultaneously a decrease of the correlation peak intensi-
ty and its shift to lower Q . The surface coalescence of
aggregates is impossible because of the strong electrostat-
ic repulsions between the charged PAA blocks. Since
nanostructures cannot rearrange themselves within the
plane, the surface pressure increase forces some copoly-
mer chains to dip from the surface to the volume. At a
given point, when this sinking frees enough space at the
surface, a better exploration of the phase space is possible
for the system. Surface strains are also relaxed. Some in-
plane reorganization may then occur. This phenomenon
is completed for surface-pressure above 8 mN/m. The
correlation peak is no longer observed and the surface
appears finally homogeneous by AFM at the highest sur-
face pressures.

Such a refined structural study performed at pH 9 com-
bined with the evolution of the isotherms on a large range
of pH demonstrates that DMF plays a huge role in the
behavior of the PS-b-PAA monolayers, whatever the pH.
It indeed extends the conclusions we obtained at pH 2
when blocks are neutral up to the charged polymer chains
case. DMF stays partially within PS blocks and is progres-
sively expelled upon compression. DMF does not com-
pletely dissolve in the water subphase but a part remains
at the surface in the monolayer due to solubility issues, as
seen previously in bulk experiments on PS-b-PAA aggre-
gates in water [24]. Then, the partition of DMF between
PS and water partially controls the behavior of the mono-
layer. Such monolayer acts thus like as a sponge with
respect to DMF. Thus, when an expansion is performed
after a compression, the DMF comes back swell the layer
as soon as the PS domains of the surface nanostructures
become accessible again. It is worth noting that the pres-
ence of DMF enables inner reorganizations within the
monolayer since PS blocks are not frozen at room tem-
perature, whereas they should be frozen without DMF (T_g
of PS is around 40°C for a molar mass of 3000 g/mol [25]).

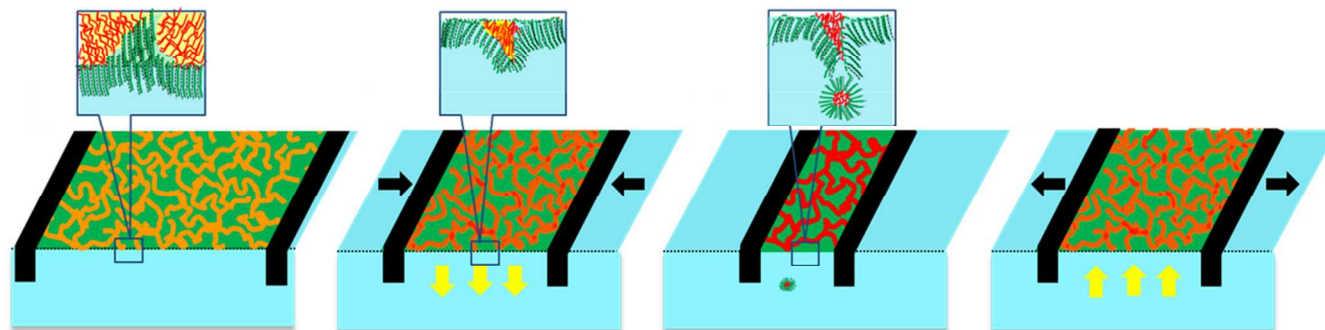


Figure 9. Schematic representations of the surface evolution of the PS-*b*-PAA at pH₉ under surface pressure variations. (PS is depicted in red domains, PAA in green domains, DMF in yellow, and water in blue. Black arrows indicate the barriers displacement and yellow arrows indicate the DMF motion. The color of PS domains changes with 2D pressure, as it depends on the amount of DMF that remains trapped inside the monolayer. The same scheme is provided in *supplementary information* from the point of view of electronic contrast.

Since PS-*b*-PAA copolymer chains are perfectly solubilized in the initial deposit solution [16], the association of chains onto the surface results from a spinodal decomposition process that occurs just after deposit during DMF removal in the out-of-equilibrium ternary system PS-*b*-PAA/DMF/water at the air/water interface. When all DMF molecules in excess have gone into water, the process is over, which fixes the characteristic wavelength and therefore the typical size of the domains. Such spinodal decomposition process is influenced by pH and solvation of PAA blocks in the subphase at the time of molecules deposit. The typical size of the domain is indeed smaller at pH 9 than at pH 2 where the uncharged PAA blocks stay adsorbed at the surface. Such typical size sets the amount of DMF that remains in the monolayer. Indeed, the experiments where pH is in situ adjusted from pH 2 to pH 9 demonstrate that less solvent molecules stay within the monolayer when the deposit is made at pH 9 than at pH 2.

Apart from the spreading solvent, electrostatic repulsions play a strong role. We remind that the ionic strength remains lower than 2.3×10^{-5} mol/L at maximum in the pH range where PAA blocks are charged ($5 < \text{pH} < 9$), *i.e.* the Debye length extends up to distances larger than 50 nm. PAA blocks are stretched and repel themselves. This is consistent with SNR that enable to recover an osmotic brush behavior. These strong repulsions make the monolayer poorly compressible and hinder in-plane reorganizations. This forces a part of the nanostructures present on the surface to be transferred from the interface to the volume when the surface pressure increases, as shown by the apparition of the second thick PS layer in SNR measurements. However, this transition from surface nanostructures to volume is reversible, as shown by GISAXS curves over several compression/decompression cycles. This reversibility suggests that the copolymer film starts buckling and deforms by creating invaginations between the interface and volume when increasing surface pressure. Indeed, if this transfer to the volume were definitive, there would be a significant loss of material, which is not observed. The loss is indeed very limited and

must take place as aggregates, presumably micelles owing to the packing parameter resulting from the ratio of the PAA to PS block units of the copolymer chains [26].

CONCLUSIONS

Our results on both subphases, pH 2 and pH 9 lead at least to the same conclusion. Contrary to most usual surfactant small molecules, the solvent used for the surface deposit plays an active role when the deposited layer consists of long amphiphilic molecules such as copolymer chains. The presence of the pseudoplateau and its evolution as function of pH is the signature of such solvent effect on the surface-pressure versus surface density isotherms. Moreover, there is a subtle interplay between the conjugate effects of spreading solvent spreading and electrostatic interactions within the monolayer that can induce structural changes. The use of neutrons and X-rays surface scattering techniques appears as a mandatory tool to probe the film behavior.

ASSOCIATED CONTENT

Supporting Information. All experimental details concerning Specular Neutron Reflectivity; all experimental details concerning GISAXS measurements; description of protocols designed to transfer the PS-*b*-PAA monolayer onto the hydrophobic wafer that ensures that sample stays maintained in liquid environment; isotherm at pH 9 over several cycles of compression/decompression; evolution of isotherms when changing the pH in situ in the subphase in order to pass from pH 2 to pH 9, respectively from pH 9 to pH 2; Table recalling the excess mass Γ obtained from SNR as function of molecular area A ; comparison of the fit of SNR data of Figure 5.a with either a one-layer model or a two-layers model; modelling of I versus Q_z at Q_{xy}^* in GISAXS experiments; modelling of the correlation peak observed in GISAXS experiment enabling to obtain its intensity and its position Q_{xy}^* ; AFM picture of the monolayer where a hole was made with the AFM tip; schematic representation of the surface evolution of the PS-*b*-PAA at pH₉ from the point of view of electronic contrast. This material is available free of charge via the Internet at <http://pubs.acs.org>.

AUTHOR INFORMATION

Corresponding Author

*E-mail: michel.goldmann@insp.upmc.fr.

*E-mail: fabrice.cousin@cea.fr.

Present Addresses

‡ Z.G.: LICORNE, ECE-Paris, 37 quai de Grenelle, 75725 Paris Cedex 15, France.

Notes

The authors declare no competing financial interest.

ACKNOWLEDGMENT

The authors thank Dr Oleg Konovalov and Dr Rana Fahra for their help during GISAXS experiments.

REFERENCES

- [1] K. Kita-Tokarczyk, M. Junginger, S. Belegriou, and A. Taubert, "Amphiphilic Polymers at Interfaces," *Adv. Polym. Sci.*, vol. 242, pp. 151–201, 2011.
- [2] E. Mouri, P. Kaewsaiha, K. Matsumoto, and H. Matsuoka, "Effect of Salt Concentration on the Nanostructure of Weak Polyacid Brush in the Amphiphilic Polymer Monolayer at the Air/Water Interface," *Langmuir*, no. 25, pp. 10604–10611, 2004.
- [3] P. Kaewsaiha, K. Matsumoto, and H. Matsuoka, "Salt Effect on the Nanostructure of Strong Polyelectrolyte Brushes in Amphiphilic Diblock Copolymer Monolayers on the Water Surface," *Langmuir*, no. 22, pp. 7065–7071, 2007.
- [4] D. Xie, C. a. Rezende, G. Liu, S. Pispas, G. Zhang, and L. T. Lee, "Effect of hydrogen-bonding complexation on the interfacial behavior of poly(isoprene)-b-poly(ethylene oxide) and poly(isoprene)-b-poly(acrylic acid) Langmuir monolayers," *J. Phys. Chem. B*, vol. 113, no. 3, pp. 739–744, 2009.
- [5] E. P. K. Currie, a. B. Sieval, G. J. Fleer, and M. a. C. Stuart, "Polyacrylic acid brushes: Surface pressure and salt-induced swelling," *Langmuir*, vol. 16, no. 22, pp. 8324–8333, 2000.
- [6] K. Ariga, Y. Yamauchi, T. Mori, and J. P. Hill, "25th Anniversary Article: What Can Be Done with the Langmuir-Blodgett Method? Recent Developments and its Critical Role in Materials Science," *Adv. Mater.*, vol. 25, pp. 6477–6512, 2013.
- [7] H. D. Bijsterbosch, V. O. de Haan, A. W. de Graaf, M. Mellema, F. A. M. Leermakers, M. A. C. Stuart, and A. A. Van Welp, "Tethered Adsorbing Chains: Neutron Reflectivity and Surface Pressure of Spread Diblock Copolymer Monolayers," *Langmuir*, vol. 11, no. 14, pp. 4467–4473, 1995.
- [8] J. K. Cox, K. Yu, B. Constantine, A. Eisenberg, and R. B. Lennox, "Polystyrene - Poly (ethylene oxide) Diblock Copolymers Form Well-Defined Surface Aggregates at the Air / Water Interface," *Langmuir*, no. 7, pp. 7714–7718, 1999.
- [9] R. B. Cheyne and M. G. Moffitt, "Novel Two-Dimensional ' Ring and Chain ' Morphologies in Langmuir - Blodgett Monolayers of PS- b -PEO Block Copolymers : Effect of Spreading Solution Concentration on Self-Assembly at the Air - Water Interface," *Langmuir*, vol. 21, pp. 5453–5460, 2005.
- [10] M. C. Faure, P. Bassereau, L. T. Lee, A. Menelle, and C. Lheveder, "Phase Transitions in Monolayers of PS - PEO Copolymer at the Air - Water Interface," *Macromolecules*, vol. 32, pp. 8538–8550, 1999.
- [11] E. P. K. Currie, a. B. Sieval, M. Avena, H. Zuilhof, E. J. R. Sudhölter, and M. a. Cohen Stuart, "Weak Polyacid Brushes: Preparation by LB Deposition and Optically Detected Titrations," *Langmuir*, vol. 15, no. 21, pp. 7116–7118, 1999.
- [12] P. Muller, G. Sudre, and O. Théodoly, "Wetting transition on hydrophobic surfaces covered by polyelectrolyte brushes," *Langmuir*, vol. 24, no. 17, pp. 9541–9550, 2008.
- [13] B. Liberelle and S. Giasson, "Friction and Normal Interaction Forces between Irreversibly Attached Weakly Charged Polymer Brushes," *Langmuir*, vol. 24, no. 4, pp. 1550–1559, 2008.
- [14] X. Wang, X. Ma, and D. Zang, "Aggregation behavior of polystyrene-b-poly(acrylic acid) at the air-water interface," *Soft Matter*, vol. 443, pp. 443–453, 2013.
- [15] O. Theodoly, a. Checco, and P. Muller, "Charged diblock copolymers at interfaces: Micelle dissociation upon compression," *EPL*, vol. 90, no. 2, p. 28004, 2010.
- [16] Z. Guennouni, F. Cousin, F. Marie-Claude, P. Perrin, D. Limagne, O. Konovalov, and M. Goldmann, "Self-organization of PS-b-PAA monolayer at the air/water interface: a process driven by the release of the solvent spreading," *Langmuir*, vol. 32, no. 8, pp. 1971–1980, 2016.
- [17] F. Cousin, F. Ott, F. Gibert, and A. Menelle, "EROS II: A boosted time-of-flight reflectometer for multi-purposes applications at the Laboratoire Léon Brillouin," *Eur. Phys. J. Plus*, vol. 126, no. 11, pp. 1–11, 2011.
- [18] Y. Han, D. Mayer, A. Offenha, and S. Ingebrandt, "Surface activation of thin silicon oxides by wet cleaning and silanization," *Thin Solid Films*, vol. 510, pp. 175–180, 2006.
- [19] T. J. Joncheray, S. A. Bernard, R. Matmour, B. Lepoittevin, R. J. El-Khoury, D. Taton, Y. Gnanou, and R. S. Duran, "Polystyrene-b-poly(tert-butyl acrylate) and polystyrene-b-poly(acrylic acid) dendrimer-like copolymers: two-dimensional self-assembly at the air-water interface," *Langmuir*, vol. 23, no. 5, pp. 2531–8, Feb. 2007.
- [20] P. Pincus, "Colloid Stabilization with Grafted Polyelectrolytes," *Macromolecules*, vol. 24, pp. 2912–2919, 1991.
- [21] E. B. Zhulina, O. V. Borisov, and T. M. Birshtein, "Structure of grafted polyelectrolyte layer," *J. Phys. II Fr.*, vol. 2, no. 1, pp. 63–74, 1992.
- [22] E. B. Zhulina and O. V. Borisov, "Structure and interaction of weakly charged polyelectrolyte brushes : Self-consistent field theory," *J. Chem. Phys.*, vol. 107, no. 15, p. 5952, 1997.
- [23] Y. Tran, P. Auroy, and L. T. Lee, "Determination of the Structure of Polyelectrolyte Brushes," *Macromolecules*, vol. 32, no. 26, pp. 8952–8964, 1999.
- [24] Y. S. Yu, L. F. Zhang, and A. Eisenberg, "Morphogenic effect of solvent on crew-cut aggregates of amphiphilic diblock copolymers," *Macromolecules*, vol. 31, no. 97, pp. 1144–1154, 1998.
- [25] T. G. Fox and P. J. Flory, "Second-Order Transition Temperatures and Related Properties of Polystyrene. I. Influence of Molecular Weight," *J. Appl. Phys.*, vol. 21, no. 6, p. 581, 1950.
- [26] Y. Mai and A. Eisenberg, "Self-assembly of block copolymers," *Chem. Soc. Rev.*, no. 41, pp. 5969–5985, 2012.

Insert Table of Contents artwork here

